AN ANALYSIS OF AC CIRCUITS AND ELECTROMAGNETISM

S. CHOURASIA
Lab Technician, Data Analyst

R. LI
Lab Technician, Data Analyst

A. LIN
Lab Technician, Data Analyst

J. YE
Lab Technician, Data Analyst

E. ZHAO
Lab Technician, Data Analyst

(Received 18 December 2019)

ABSTRACT

Four different experiments were carried out in order to investigate RC and CLR circuits, transformers, and solenoid magnetic fields. The phase shift of the RC circuit was found to be (-75.6±.9)°, while the resonant frequency of the CLR circuit was found to be (160±20) Hz. Both values conformed with theory. The primary source of potential loss in the transformer as frequency increased was suggested to be hysteresis loss. In the solenoid experiment, magnetic field data was compared to theoretical values, and the relatively large residuals near the centre of the solenoid were attributed to the theory equation's inaccuracy for solenoids with nontrivial thickness. This was extended to a rendering of magnetic field interactions with two solenoids. O-C residuals between computed and collected data showed a consistent difference in magnitude between values, such that the field travels in the correct directions as calculated but with weaker magnitude.

I INTRODUCTION

While direct current has many uses, most notably in batteries, alternating current (AC) is significantly more economical across long distances. Furthermore, AC can be easily modified using devices such as transformers. Thus, AC is extremely prevalent in homes. In addition, the flow of electric current is largely related to magnetic fields. The properties of both AC and any related magnetic fields are increasingly significant in the modern way of life and can be more clearly understood in an exploration of their behaviour using various devices.

II THEORY

The impedances of a capacitor or inductor with an AC source are, respectively:

$$X_c = \frac{1}{2\pi f C} \quad [1]$$

(HRW, 2011)

$$X_L = 2\pi f L \quad [2]$$

(HRW, 2011)

Where:

f = Frequency of AC current (Hz)
X_C = Capacitive reactance of the capacitor (Ω)
C = Capacitance of the capacitor (F)
X_L = Inductive reactance of the inductor (Ω)
L = Inductance of the inductor (H)

The phase shift of an RLC circuit is:

$$\tan\phi = \frac{X_L - X_C}{R} \quad [3]$$

(HRW, 2011)

Where:

ϕ = Phase constant (rad)
R = Resistance in the circuit (Ω)

The impedance of an RLC circuit is:

$$Z = \sqrt{R^2 + (X_L - X_C)^2} \quad [4]$$

(HRW, 2011)

Where:

Z = Impedance in the circuit (Ω)

The output impedance of a function generator can be found using the following:

$$Z_0 = R_L\left(\frac{V_0 - V_L}{V_L}\right) \quad [5]$$

(Collinson, 2019)

Where:

Z_0 = Impedance of function generator (Ω)
R_L = A known resistance (Ω)
V_0 = Potential measured over open circuit (V)
V_L = Potential across known resistor in series (V)

Resonance of an RLC circuit occurs at:

$$f = \frac{1}{2\pi\sqrt{LC}} \quad [6]$$

(HRW, 2011)

The electromotive forces across the two ends of a transformer are given by:

$$\frac{\xi_1}{N_1} = \frac{\xi_2}{N_2} \quad [7]$$

(HRW, 2011)

Where:

ξ_i = emf of the i^{th} end (V)
N_i = Number of turns of the i^{th} end

The magnetic field along the longitudinal axis of a thin coil is given by:

$$B(z) = \frac{\mu_0 NI}{4h}\left(\frac{h-z}{\sqrt{R^2+(h-z)^2}} + \frac{h+z}{\sqrt{R^2+(h+z)^2}}\right) \quad [8]$$

(Calaghan, 1960)

Where:

B = Magnetic field (T)
z = Distance from centre of coil (m)
h = Half of solenoid length (m)
$\mu_0 = 4\pi \times 10^{-7}$ = Vacuum Permeability (Hm^{-1})
N = Number of turns in the coil
I = Current (A)
R = Radius of coil (m)

III Method

A 1 mF capacitor, 10 kΩ resistor, and 12 Ω resistor were acquired pursuant to van Bemmel (2019). A BK Precision 5 MHz Function Generator Model 4011A was the AC source, while electric potential was found with a Tektronix 1052B Oscilloscope. Multimeters and Vernier Hall effect probes were used to find resistance and magnetic field, respectively. To verify performance, three of each device were used to effect the same measurement; they were deemed functional if the readings were within a range of ten times the stated resolution.

For the first experiment, a series RC circuit was constructed with the components from Lab 3, in accordance to Fig 1.

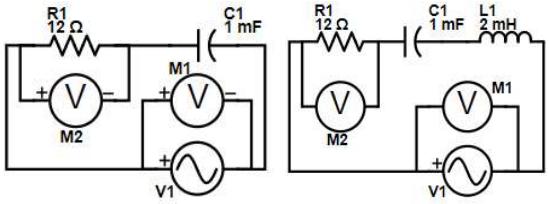

Fig 1. RC and RLC Circuits. The above schematics were used for circuit 1 (left) and circuit 2 (right). The noted values are manufacturer values for each component's properties. The potential of the AC source is omitted as it varied based on the circuit impedance.

To encourage a sensible phase shift, a second RC circuit with a 12 Ω resistor was built. Potentials of the function generator across the open circuit and across a known resistor R_L were taken to find R_0, the internal resistance of the source, which was considered in the further analysis. Also, impedance matching could be achieved.

Then, a series RLC circuit was built as shown in Fig 1. Potential across the function generator was measured against frequency as described by van Bemmel (2019).

For the third experiment, a transformer was created using a magnetic core, 300 $Wdgm^{-1}$ solenoid, and a 1200 $Wdgm^{-1}$ solenoid. The transformer was connected to a resistor, function generator and oscilloscope. Potential probes took measurements across the function generator and resistor to find the input and output potentials, respectively.

In the fourth experiment, a Hall effect probe was attached to a cart with tape along the longitudinal axis of the Helmholtz coil. A minimum distance of 0.5 m from other electronic devices was maintained to minimize their effect on the probe. The magnetic field was measured at every increment of 5 mm. A measurement was taken without a current to find the magnitude

of the background field, which could then be uniformly subtracted from the measurements to find the solenoid's magnetic field.

For the extension, two Helmholtz coils with slightly different currents were oriented asymmetrically. The Hall effect probe was taped onto wooden blocks to maintain a static position while measurements were taken. It was then set at six different points, taking measurements along multiple axes for each point by bending the tip of the probe and adjusting the location to ensure that the tip was at the same location each time.

IV Data

The following data was taken for the internal impedance of the function generator:

Index	Value	Amplitude of AC Potential (V)
1	V_0	11.1±.1
2	V_L	2.2±.1

Fig 2. Potentials of Function Generator. Measured potentials of the function generator for circuit 1, as taken across an open circuit (V_0) and a known resistor R_L (V_L). R_L had a measured resistance of (12.3±.1) Ω.

A resistor of (12.3±.1) Ω was used in the RLC circuit. The inductor and capacitor were listed at 2 mH and 1 mF, respectively.

Circuit 3 used the following coils:

Solenoid	Variable Name	Number of Turns
1	N_1	300
2	N_2	1200

Fig 3. Transformer Data. The number of turns made by each coil used in the transformer. The expected ratio of input to output potentials is 4, the quotient of N_2 divided by N_1.

The properties of the solenoid are:

Index	Property	Measured Value
1	Resistance	6.7±.1 Ω
2	Potential	1.21±.1 V
3	Coil Width	(0.020±.2) m
4	Coil Radius	(0.136±.3) m
5	Number of Windings	320±1

Fig 4. Solenoid Measurements. The following measurements were taken for the circuit containing a Helmholtz coil. All measurements are assumed to be constant during the measurement of the magnetic field.

V Analysis

Finding the impedance of the function generator, the values from Fig 2 were substituted into [5], yielding an impedance of (49±5) Ω. This value will be considered in the further analysis of the CLR circuits.

From [1] and [3], the phase shift of an RC circuit increases as frequency decreases. However, substituting the values of the RC circuit from Lab 3, namely a resistance of 10 kΩ and capacitance of 1 mF, with a frequency of 2.5 Hz, into [3] yields a theoretical phase shift of -0.365°. To confirm this, potential and current were taken across the resistor and a Lissajous figure was made:

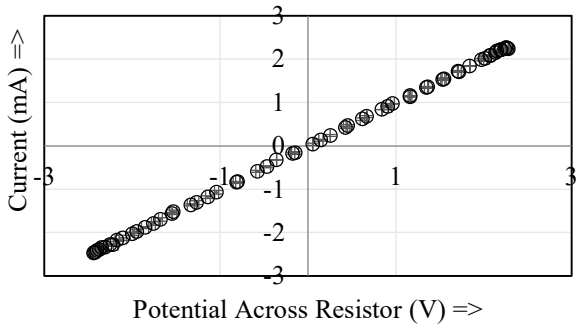

Fig 5. Lissajous Figure with 10 kΩ resistor. The plot of potential versus current with a 10 kΩ resistor forms a Lissajous figure resembling a straight line, indicating a negligible phase shift. 2.5% of the data is shown.

The same experiment was conducted using a 12 Ω resistor to promote a phase shift, as well as impedance matching. Impedance matching occurs when the circuit impedance matches that of the source (Frenzel, 2011). [4] can then be used to solve for capacitive impedance. Substituting known values yields a capacitive impedance of (51±5) Ω. Then, from [1] and [6], the impedance-matching frequency of (3.3±.7) Hz was calculated. Then, substituting the calculated frequency and given RC circuit values into [3] yields a phase shift of (-76±1)°. Using a signal with a frequency of (3.3±.1) Hz, then by finding the linear fit of the sine inverse of the waveform, it was then found that the constructed circuit's phase shift is (-75.6±.9)°, which is comparable to the theoretical value. A

Lissajous figure was then constructed for the potential versus current of the new RC circuit to confirm conformity to theory.

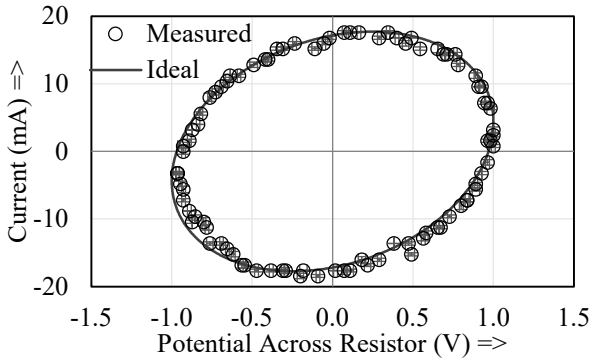

Fig 6. Lissajous Figure with 12 Ω resistor. The Lissajous figure of an RC circuit with a 12 Ω resistor forms an ellipse, indicating a significant shift. The signal is plotted against the calculated shift, using the same amplitude for AC potential and current. 5% of the data is shown.

Following this, an LR circuit was constructed to measure the properties of an inductor. The measured data of the potential and current waveforms is shown below:

Property	Potential of Waveform	Current of Waveform
Frequency (Hz)	5609±1	5609±1
Amplitude	(1.17±.06) V	(0.23±.2) A
Shift from 0° (°)	60.0±.4	-11.4±.3

Fig 7. LR Circuit Measurements. The measured values for the current and potential in an LR circuit. Shift from 0° was calculated by linearly regressing the inverse sine function of the wave equation. These values are then used to calculate the properties of an inductor.

The difference in shifts from Fig 7 yields a total of (71.4±.5)°. Then, substituting this into [3], and using it with [2], one can calculate the inductance within the circuit. A similar analysis was conducted on Circuit 1 to measure the capacitance with [1].

X_L (Ω)	L (mH)	C (mF)
37±1	1.06±.03	1.0±.1

Fig 8. CLR Circuit Measurements. The measured values for the inductor and capacitor are shown, calculated by the methods described above.

Thus, the theoretical resonant frequency can be found from [6] to be (150±10) Hz.

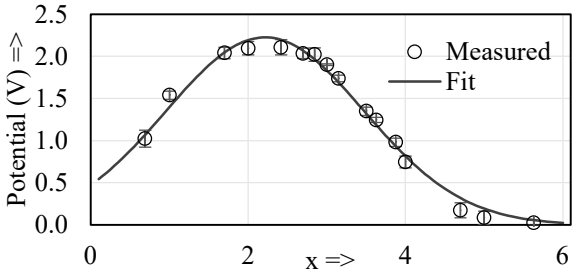

Fig 9. RLC Amplitude vs. Frequency Order of Magnitude. The amplitude of potential across the resistor as a function of x, the exponent to which 10 must be raised to equal the measured frequency. On this logarithmic scale, the data can be empirically modelled using a Gaussian function.

Fig 9 shows the measured electric potential data versus frequency on a logarithmic scale. It is shown that the amplitude can be approximated by a Gaussian function, which is utilized for its symmetry. This enables the calculation of a resonant frequency. Using a logarithmic scale, it is shown that the fit has an R^2 value of 0.99. From this, the Gaussian empirical model was assessed to be suitable for a mathematical analysis of the curve. It was found that the curve had a central value of (2.21±.06). The scale was converted from logarithmic to linear, and a resonant frequency of (160±20) Hz was found. This value is within the confidence range of the expected value, thus conforming to theory.

Data from the third circuit was used to find the ratio of potentials for each frequency. An exponential fit was empirically determined to be optimal for the data.

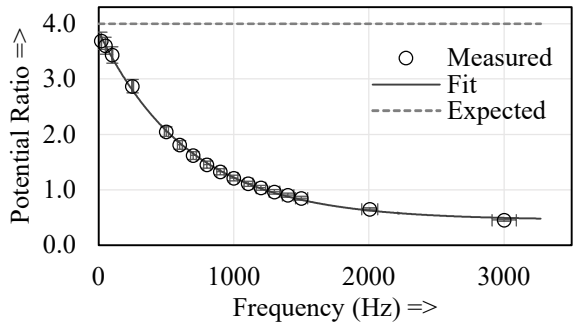

Fig 10. Frequency vs Potential Ratio. The measured ratio of input to output potential, fit empirically using an exponential function. The potential loss compared to the expected value can be attributed to hysteresis and eddy current losses. The resulting R^2 value was 0.99.

It is suggested that the most significant contributors to potential loss were hysteresis, eddy current, and copper loss. These all serve to reduce the amount of power across the second end of the transformer. It should be noted that power is proportional to the square of potential, and therefore power losses also create potential loss. Hysteresis loss occurs due to rapid switching of the current directions, causing the core to cycle between states of magnetization and demagnetization. Eddy current losses are caused by induced emf, which create currents to circulate in the core, and copper loss is loss due to heat.

It was determined that hysteresis loss was the dominant mechanism of power loss, as it satisfies a power law of degree -0.6 with respect to frequency (Collins, 2018). This explains the power loss's decreasing rate of change as it levels off at higher frequencies.

Magnetic field data from the Hall effect probe in the fourth experiment was plotted against the distance of the end of the probe from the coil centre. The theoretical magnetic field with respect to distance was found with [8]. These values are shown in Fig 11.

It is noted that the measured values depict the same symmetry that is expected from theory, indicating some level of conformity. However, it was seen that there are residuals in the calculation. This is most apparent at the centre of the solenoid, where the theoretical field strength is (447±1) μT, compared to the measured (364±2) μT.

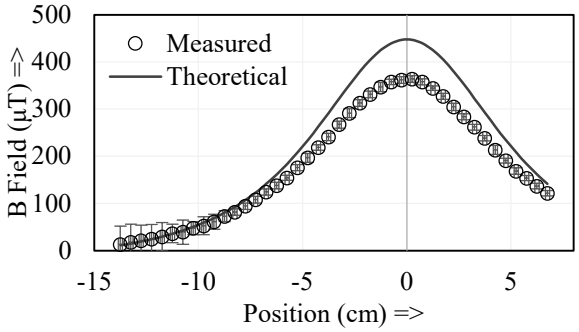

Fig 11. B Field vs Position Relative to Centre. The theoretical and measured values for the magnetic field along the solenoid's longitudinal axis are plotted. Theoretical values are pursuant to [8]. The resulting R^2 value was 0.99.

It is postulated that this is due to the equation in [8] being a simplification of the actual magnetic field along the solenoid, assuming negligible thickness of the solenoid. In reality the solenoid thickness was a nontrivial (2.0±.2) cm. This would also explain the greater significance of the discrepancies near the middle of the coil, where the approximation is more inaccurate.

For the extension, software was created using MATLAB pursuant to van Bemmel (2005) to provide calculated magnetic field values by the Biot-Savart Law (BSL). The program involved a second solenoid which was arbitrarily angled 68° relative to the first and translated at a slant. The solenoids were discretized such that they would each be composed of a set number of points in a helix.

A range of coordinates were then selected for which the magnetic field vector would be found. In order to integrate BSL to compute **B**, each point of reference **P** would sum the d**B** vectors found using the law. The **r** vector was computed as the displacement from **P** to the solenoid points, and the d**s** vector took the vector difference between consecutive solenoid points for a Riemann Sum. The **B** vectors are streamlined with a built-in function to show their flow.

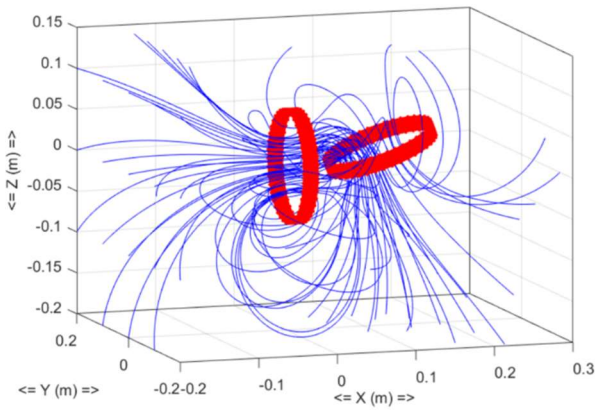

Fig 12. 3-D Plot of Magnetic Field Lines. The magnetic field lines, which flow in the negative-x direction (right-to-left), are shown through two solenoids. The right solenoid has a translation of (x,y,z) = (13,4,2) cm approximately.

An experimental setup with two solenoids in known orientations was then

assessed at 6 unique points to then compare with the program's calculated field strength.

Point, Axis	Observed (mT)	Calculated (mT)	O-C Residual
1, x	-0.156±.001	-0.294	0.064±.001
1, y	0.045±.001	0.0505	-0.005±.001
1, z	-0.044±.001	-0.0631	0.019±.001
2, x	-0.193±.001	-0.317	0.124±.001
2, y	0.037±.001	0.0461	-0.009±.001
2, z	-0.018±.002	-0.0218	0.004±.002

Fig 13. O-C of Magnetic Field Software. A comparison of the calculated values for the field strength to the measured field strength at the specified points and axes. The two featured points are (-6.2, -4.2, 0) and (-6.2, -2.2, 0) cm, with each dimension having an uncertainty of ±.2 cm. Similar results are attained with the other four points.

The observed values are all consistently lesser in magnitude than calculated, indicating that the magnitude of the induced field is not as strong as assumed in theory. As the BSL relies on factors such as position and sum approximations which are difficult to precisely give, a skewed approximation may consistently increase calculated values. Inaccurate position measurements relative to the origin would also cause such a residual. Aside from this, the observations mostly agree with the accepted BSL situation to the same degree of magnitude.

VI Sources of Error

When performing measurements of magnetic field for the extension, it was noticed that the batteries used to power the solenoid slightly decreased in potential after the lab session. Since magnetic field is linearly dependent on current by [8], which is linearly dependent on potential by Ohm's Law (HRW, 2011), the measurements taken later may have had lower magnetic fields than predicted. Further, minor magnetic fields stemming from devices such as batteries and probes likely added to or changed the ambient field, despite efforts to reduce this. A similar setup was utilized for the fourth experiment, and may have also been subject to these sources of error.

VII Conclusion

In the first experiment, a series RC circuit with impedance matching was made to ensure a proper Lissajous figure. The phase shift was found to be (-75.6±.9)°, which is in the theoretical range of (-76±1)°.

In the second experiment, the inverse sine of the data was linearly fit. A resonant frequency of (160±20) Hz was found, conforming to the predicted (150±10) Hz.

In the third experiment, the ratios of potential at both ends were empirically fitted to an exponential curve. It was postulated that the loss was primarily due to hysteresis loss, which conforms with the ratio approaching asymptotic behaviour at high frequencies.

In the fourth experiment, the magnetic fields along the longitudinal axis of a Helmholtz coil was compared with theoretical values. Significant residuals were observed near the centre of the solenoid, where [8] would produce greater inaccuracies. Extending this, a program was written to model two solenoids. Comparisons with measurements show calculated values are consistently greater, indicating a possible bias of either the code or the measurements.

VIII Sources

van Bemmel, H., "AP Physics C Laboratory Manual", http://www.hmvb.org/apc1920lm.pdf, 2019

[2], "Lab 4 – Off Axis B Fields", http://www.hmvb.org/biotsav art.pdf, 2005

BK, "4010A & 4011 data sheet", https://bkpmedia.s3 .amazonaws.com/downloads/datasheets/en-us/401xA _datasheet.pdf, 2018

Calaghan, E., Maslen, H., "The Magnetic Field of a Finite Solenoid", https://ntrs.nasa.gov/archive/nasa/casi .ntrs.nasa.gov/19980227402.pdf, 1960

Collins, D., "Hysteresis Loss", https://www.motioncontrolti ps.com/hysteresis-loss/, 2018

Collinson, A. "Measuring Input and Output Impedance", http://www.zen22142.zen.co.uk/Theory/inzoz.htm, 2019

Frenzel, L. "Back to Basics: Impedance Matching", https://www.electronicdesign.com/technologies/com munications/article/21796367/back-to-basics- impedance-matching-part-1, 2011

Halliday, D., Resnick, R., Walker, J. (HRW), Fundamentals of Physics 9e, Wiley, 2011s